Fish and Shellfish Immunology 84 (2019) 521–531

Contents lists available at ScienceDirect

Fish and Shellfish Immunology

journal homepage: www.elsevier.com/locate/fsi

Full length article

Transcriptome profiling reveals key roles of phagosome and NOD-like receptor pathway in spotting diseased *Strongylocentrotus intermedius*

Weijie Zhang[a,b], Zhimeng Lv[a], Chenghua Li[a,*], Yahui Sun[b], Huijie Jiang[b], Manxi Zhao[b], Xuelin Zhao[a], Yina Shao[a], Yaqing Chang[b,**]

[a] School of Marine Sciences, Ningbo University, Ningbo, Zhejiang Province, 315211, PR China
[b] Key Laboratory of Mariculture & Stock Enhancement in North China's Sea, Ministry of Agriculture and Rural Affairs, Dalian Ocean University, Dalian, 116023, PR China

ARTICLE INFO

Keywords:
Strongylocentrotus intermedius
Transcriptome
Spotting disease
qPCR

ABSTRACT

Spotting disease is a common disease in the process of aquaculture and restocking of the sea urchin *Strongylocentrotus intermedius* and leads to mass mortality. To characterize the molecular processes and candidate genes related to spotting disease in *S. intermedius*, we conducted next-generation sequencing to assess the key genes/pathways in spotting diseased sea urchin (DUG) compared to healthy ones (HUG). A total of 321.1 million clean reads were obtained and assembled into 93,877 Unigenes with an N50 of 1185 bp, in which 86.48% of them matched to the genome sequence of the sea urchin *S. purpuratus* and 27,456 Unigenes mapped to Nr database. Salmon expression analysis revealed 1557 significantly differently expressed genes (DEGs) between DUG and HUG. These DEGs were enriched into 151 KEGG pathways including a core set of immune correlated pathways notably in phagosome and NOD-like receptor signaling. DUG displayed an obvious downregulation in these immune pathways. The expression patterns of six DEGs were confirmed by RT-qPCR, and the expressions were consistent with the results of RNA-seq. Furthermore, 15,990 SSRs were identified and a total of 235,249 and 295,567 candidate SNPs were identified from DUG and HUG, respectively. All these results provided basic information for our understanding of spotting disease outbreak in sea urchin.

1. Introduction

The sea urchin *Strongylocentrotus intermedius* was originally found off the coastal of North Japan and Far East of Russia [1]. It was introduced from Japan into China in 1989 for its fast growth rate and high quality roe [2,3]. Since then, lots of studies have been conducted on its biology, ecology, aquaculture and genetic and breeding [4–11]. Benefited from these researches, *S. intermedius* has become the main cultured sea urchin species in China now. Over 20 million artificial seeds and 1000 mt live *S. intermedius* are produced yearly in China. With the development of its aquaculture industry, infectious diseases in either juveniles in hatcheries or adults in aquaculture farms are commonly observed and occasionally lead to mass mortality [12–18].

Spotting disease is a common disease in the process of aquaculture and restocking of *S. intermedius* [12,13,16–18]. The diseased sea urchins have spotting lesions with red, purple or blackish color on the body wall followed by the detachment of local spines (Fig. 1). The progressively enlarging spotting lesions will cause ulceration on the body wall and finally lead to death. Spotting disease results in mass mortality in aquaculture of *S. intermedius* and brings huge economic losses [13,16–18]. Therefore, establishing an effective disease control strategy will throw new insights on the species aquaculture. It is recognized that bacteria are the major pathogen of spotting disease. However, which bacterium is the causative pathogen is controversial. Tajima et al. [12,13] isolated a filiform bacterium that belonged to the genus *Flexibacter* from the spotting diseased *S. intermedius* and proved that it was the causative bacterium. However, Wang et al. [18] isolated two dominant bacteria and proved one of them that belonged to the genus *Vibrio* was the causative bacterium. Despite the difference, Tajima et al. [13] and Wang et al. [18] reported the same season (in summer when the seawater temperature rises over 20 °C) when the spotting disease outbroke and they also made an identical conclusion namely the high water temperature promoted the reproduction of the causative bacteria, and under this condition, those sea urchins who had physically injury were easily infected. Based on these analysis, lowering the water temperature or reducing the physical injury should be useful in preventing the spotting disease. However, high temperature and physical injury are always unavoidable in sea urchin aquaculture. So, to

* Corresponding author. 818 Fenghua Road, Ningbo University, Ningbo, Zhejiang Province, 315211, PR China.
** Corresponding author. 52 Heishijiao Street, Dalian Ocean University, Dalian, Liaoning Province, 116023, PR China.
E-mail addresses: lichenghua@nbu.edu.cn (C. Li), yqchang@dlou.edu.cn (Y. Chang).

https://doi.org/10.1016/j.fsi.2018.10.042
Received 21 June 2018; Received in revised form 13 August 2018; Accepted 16 October 2018
Available online 17 October 2018
1050-4648/

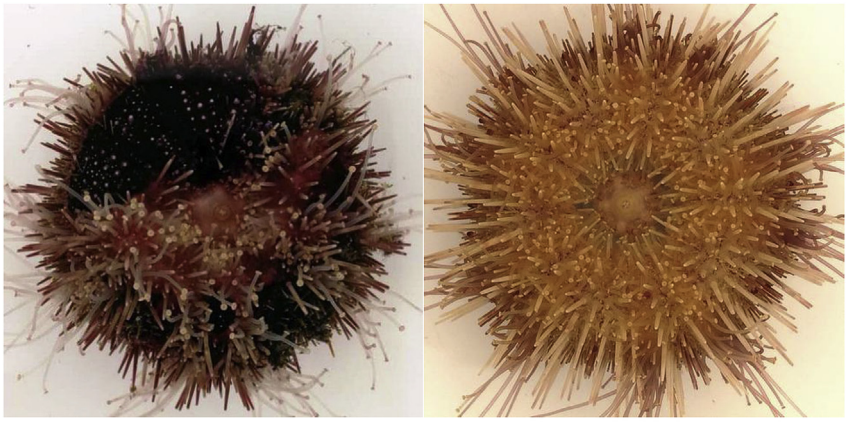

a b

Fig. 1. Symptom observation of spotting diseased and healthy *Strongylocentrotus intermedius*. a: spotting diseased sea urchin; b: healthy sea urchin.

Table 1
List of primers used for RT-qPCR validation.

Gene name (abbreviation)	Gene name (official full name)	Forward primer (5′-3′) and Reverse primer (5′-3′)	TM (°C)	Amplicon length (bp)
CASP8	Caspase-8-like	CCCTCTCTTGTGGGCAAACC	59.3	279
		TGCATGACTCATCCGCTCGT	59.4	
NCAN	Neurocan core protein	CTGGACCGATGGAAAACCG	56.6	266
		TGAAGCAGGAGTCGCCGTAT	58.9	
STY46	Serine/threonine-protein kinase	CGCACTACTAAATGGCAACAGC	56.9	229
		GACTGTCCGTGCCCCAACAC	62.3	
TIGAR	Fructose-2,6-bisphosphatase	GGAGACAAGGAGGGGATTACG	57.5	145
		TGCAGATGTCGTGGAAGGCT	59.5	
TRAF3	TNF receptor-associated factor 3	TCCTGCGTCCTGTCATTCTCA	58.4	143
		ACTGCTGTTGGGGTCTGGTTG	60.6	
TRIM30a	Tripartite motif-containing protein 30A	CCTGGCAGTCCTTTTCACCC	59.3	250
		CCATTTTCCACATCCCAACACC	56.8	
β-actin	*β*-actin	AGAGGCGTAGAGGGAAAGAC	56.4	92
		ACAGGGAAAAGATGGCACAGA	56.4	

Table 2
Summary of the four *S. intermedius* transcriptome.

Sample	Raw_Reads	Valid_Reads	Ratio
DUG1	80,718,574	79,611,864	98.63
DUG2	77,856,728	76,741,382	98.57
HUG1	87,731,720	86,623,618	98.74
HUG2	79,371,532	78,145,348	98.46
Total	325,678,554	321,122,212	

Table 3
Basic information of assembled transcriptome.

Index	All	GC%	Min length	Max length	N50 length
Transcript	215,164	39.55	201	16712	1147
Unigene	93,877	39.64	201	16712	1185

develop spotting disease resistant strains might be a promising way in the practice of *S. intermedius* culture.

Due to lack of adaptive immune system, sea urchins rely on innate immune system to defense against pathogenic microbial infection. An elaborate repertoire of genes related to immunity such as Toll-like receptors (TLR), NACHT and leucine rich repeat containing (NLR) genes have been revealed by the genome sequence of another species *S. purpuratus* [19]. In addition, a large and diverse set of sp185/333 genes have been identified to be involved in the immune response to LPS injection in *S. purpuratus* using differential display and subtracted probes followed by EST analysis [20]. Single innate immune-related genes have been identified and proven to be involved in the process of immune regulation in relation to bacterial infection. For examples, expression of Sp064 gene which encodes SpC3 increased significantly in plutei of *S. purpuratus* which were cultured in the presence of heat-killed bacteria *Vibrio diazatrophicus* [21]. Compared to the rich genomic resource in *S. purpuratus*, only 185/333 family gene (*Si185/333-1*) [22,23] and TLR11 family gene (*SiTLR11*) [24] were characterized in *S. intermedius*. Herein, high-through RNA-seq was performed in spotting diseased and healthy *S. intermedius* coelomocytes using Illumina Hiseq 4000 platform. We aimed to clarify key signal transduction pathways involved in immune defense against spotting disease infection at transcriptome level, which may provide a better insight into sea urchin immunity mechanism. These data should be very helpful to develop disease control strategy in aquaculture and selective breeding of sea urchins.

2. Materials and methods

2.1. Samples preparation and RNA extraction

Sea urchins *S. intermedius* were cultured in our lab of Key Laboratory of Mariculture and Stock Enhancement in North China's Sea, Ministry of Agriculture and Rural Affairs, Dalian Ocean University, China. On 15th August, 2017, spotting diseased individuals was firstly observed in the cultured sea urchin population. When the percentage of diseased individuals were around 50% on 1st September, 2017, four diseased and four healthy sea urchins of the same size (53.4 ± 2.9 mm in diameter) were collected. Coelomic fluid from each individual was sampled and centrifuged immediately at 500 × *g* for 10 min at 4 °C to harvest the coelomocytes. The coelomocytes of each sea urchin was immediately

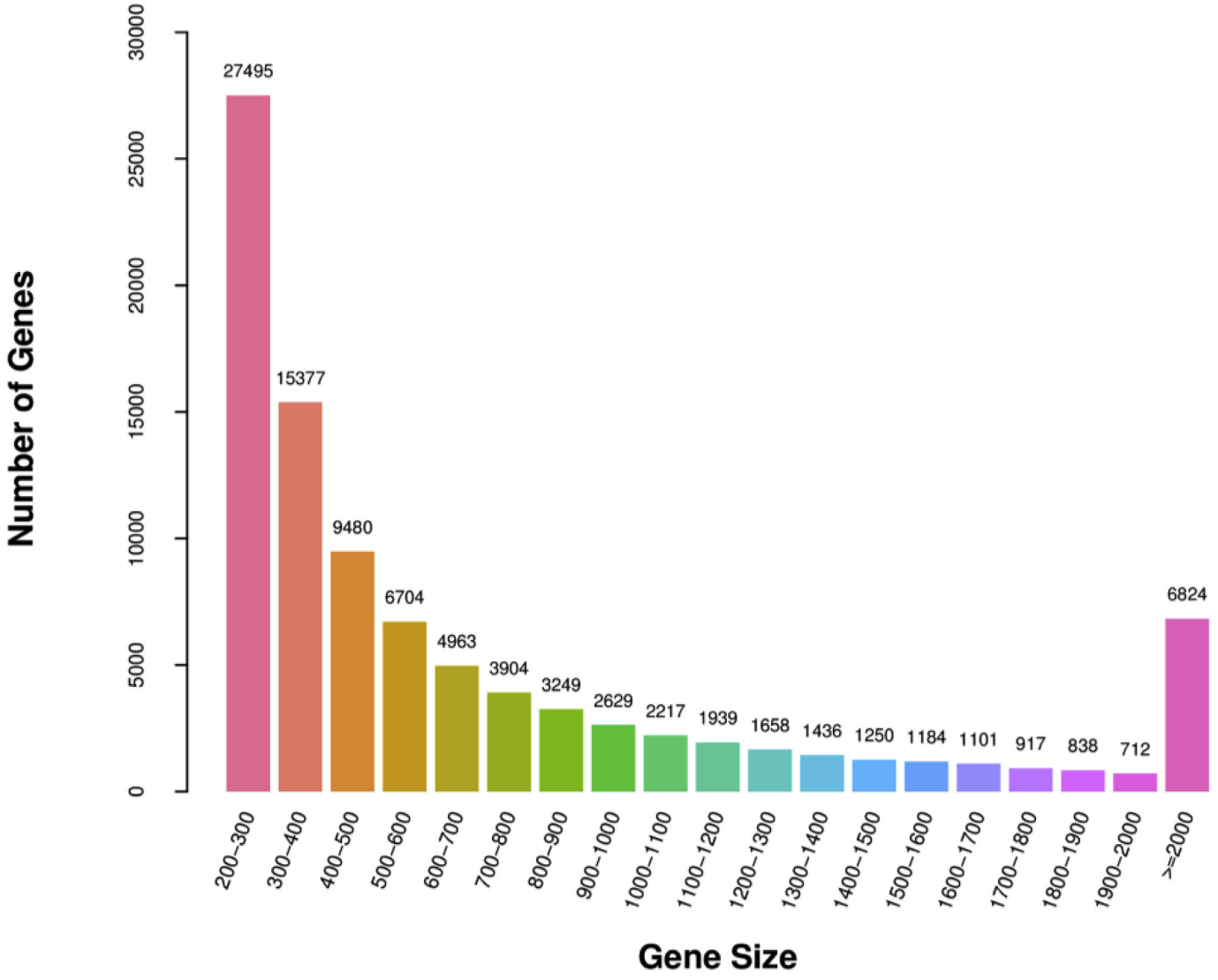

Fig. 2. Length distribution of assembled transcripts for all unigenes.

Table 4
Statistics of annotation results of Unigenes.

DB	Num
All	93,877
Nr	27,456
GO	19,905
KEGG	11,558
Pfam	18,049
Swissprot	14,960
eggNOG	30,099

snap-frozen in liquid nitrogen and then stored at −80 °C. Total RNA was extracted using Trizol reagent (Invitrogen, CA, USA) following the manufacturer's procedure. The RNA quantity and purity were analyzed by Bioanalyzer 2100 and RNA 6000 Nano LabChip Kit (Agilent, CA, USA) with RIN number > 7.0.

2.2. cDNA library construction and sequencing

Equal amounts of RNA (5 μg) from two individuals in diseased urchin group (DUG) or healthy urchin group (HUG) were pooled together as one replicate for RNA-Seq library construction as follows. Samples from each group were subjected to isolate Poly (A) mRNA with poly-T oligo attached magnetic beads (Invitrogen). Following purification, the poly(A)- or poly(A)+ RNA fractions is fragmented into small pieces using divalent cations under elevated temperature. Then the cleaved RNA fragments were reverse-transcribed to create the final cDNA library in accordance with the protocol for the mRNA-Seq sample preparation kit (Illumina, San Diego, USA). The paired-end sequencing was performed on an Illumina Hiseq 4000 following the vendor's recommended protocol.

2.3. Transcriptome assembly

Firstly, Cutadapt [25] and perl scripts in house were used to remove the reads that contained adaptor contamination, low quality bases and undetermined bases. Then sequence quality was verified using FastQC (http://www.bioinformatics.babraham.ac.uk/projects/fastqc/) including the Q20, Q30 and GC-content of the clean data. All downstream analyses were based on clean data of high quality. De novo assembly of the transcriptome was performed with Trinity 2.4.0 [26]. Trinity groups transcripts were clustered based on shared sequence content. Such a transcript cluster was very loosely referred to as a 'gene'. The longest transcript in the cluster was chosen as the 'gene' sequence (aka Unigene).

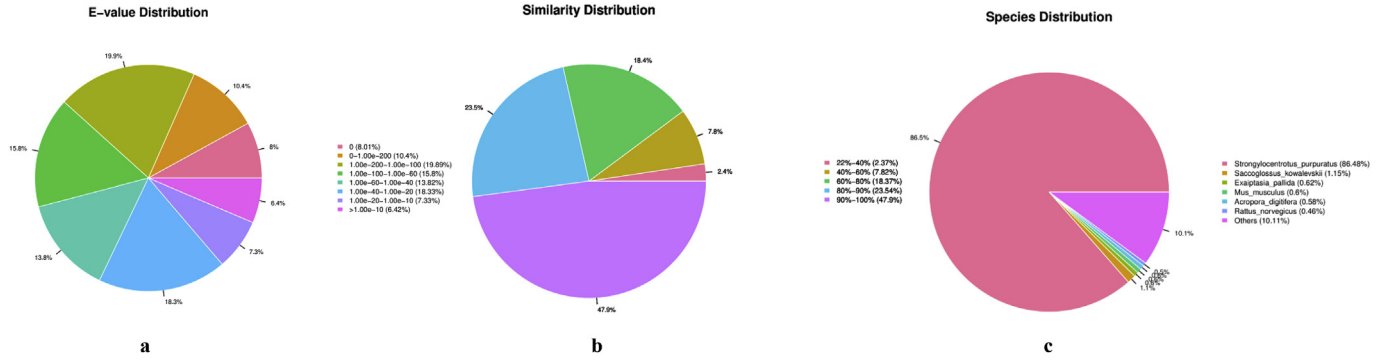

Fig. 3. Statistics of species with DIAMOND results in Nr database. a: E-value distribution of BlastX hits with a cut-off E-value of 10^{-5}. b: Similarity distribution of the closest BlastX matches for each sequence. c: Species based distribution of BlastX matches for sequences.

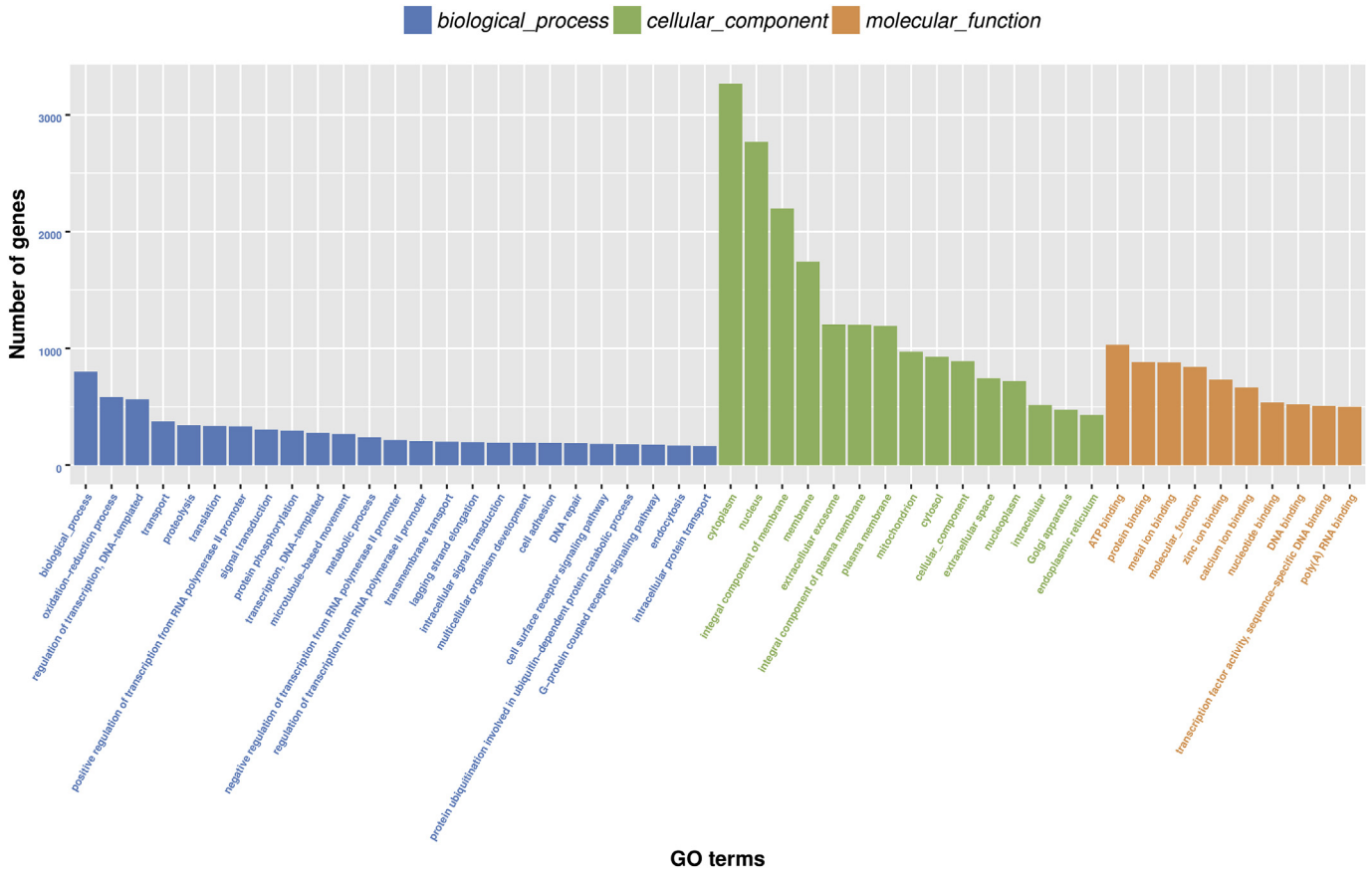

Fig. 4. Functional annotation of genes based on GO categorization.

2.4. Gene annotation

All assembled Unigenes were aligned against the non-redundant (Nr) protein database (http://www.ncbi.nlm.nih.gov/), Gene ontology (GO) (http://www.geneontology.org), SwissProt (http://www.expasy.ch/sprot/), Kyoto Encyclopedia of Genes and Genomes (KEGG) (http://www.genome.jp/kegg/) and eggNOG (http://eggnogdb.embl.de/) databases using DIAMOND [27] with a threshold of E-value < 0.00001.

2.5. Differential expression analysis

Salmon [28] was used to perform expression level for Unigenes by calculating TPM (Transcripts Per Million) [29]. The differentially expressed Unigenes (DEG) were selected with log2 (fold change) > 1 or log2 (fold change) < -1 with statistical significance (p value < 0.05) by R package edgeR [30]. Next, GO and KEGG enrichments were performed on the differentially expressed Unigenes by perl scripts in house.

2.6. Validation DGEs by RT-qPCR

Six DEGs were selected for RT-qPCR validation, and the unigenes information was showed in Table 1. RNA used for RT-qPCR amplifications were the same with those used to construct cDNA library. Gene-specific primers were designed based on the transcriptome sequences using Primer Premier 5.0. The primer sequences are listed in Table 1. Differential expressed genes analysis was performed using ABI 7500 real-time PCR detection system. Real-time PCR amplification was performed in a 20 μL reaction containing 10 μL 2 × SYBR Green Mix (TaKaRa), 8 μL diluted cDNA (1:100), 0.8 μL of each primer (10 mM) and 0.4 μL of ROX. The following qPCR parameters were used: (1)

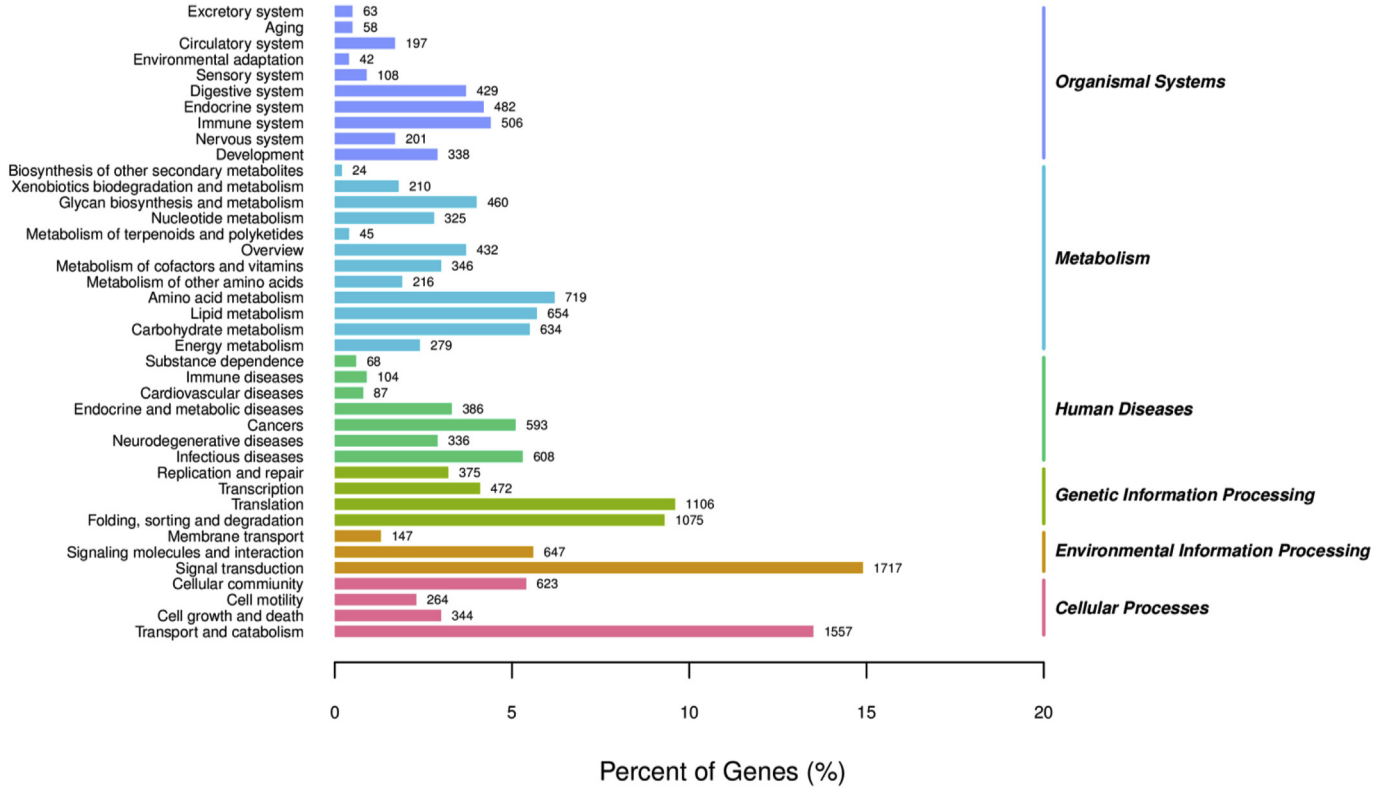

Fig. 5. Pathway enrichment of all annotated unigenes by KEGG analysis.

denaturing step at 95 °C for 3 min; (2) 40 cycles of 95 °C for 15 s and 60 °C for 1min. The relative quantities of the target genes were calculated using *β*-actin from *S. intermedius* as endogenous control gene according to the $2^{-\Delta\Delta C_T}$ method [31]. The difference in each gene expression between DUG and HUG were compared using paired-samples. Significant level was set as $P < 0.05$.

2.7. Discovery of SSR and SNP

MISA software (http://pgrc.ipk-gatersleben.de/misa/) was used to detect putative SSRs from the assembled transcriptome. The parameters were adjusted to identify mono-, di-, tri, tetra-, penta- and hexa-nucleotide motifs with a minimum of 12, 6, 5, 5, 4 and 4 repeats, respectively. The candidate SNPs were analyzed with Bowtie software.

3. Results

3.1. Sequencing and unigenes assembly

Four *S. intermedius* cDNA libraries with two diseased groups and two control groups were constructed. A total of 325,678,554 raw reads were obtained using an Illumina Hiseq 4000 system. After discarding the low-quality reads, 321,122,212 clean reads were obtained and used for *de novo* assembly (Table 2). The high-quality reads were deposited in the short read archive of NCBI under the accession number SRR7701064, SRR7701065, SRR7701066 and SRR7701067.

A total of 215,164 transcripts range from 201 bp to 16,712 bp with an N50 of 1147 bp were assembled for *S. intermedius*. A total of 93,877 Unigenes range from 201 bp to 16,712 bp with an N50 of 1185 bp were assembled (Table 3). The detailed length distribution of the transcripts is shown in Fig. 2.

3.2. Functional annotation of unigenes

All Unigenes against GO, KEGG, Pfam, Swissprot, eggNOG and Nr databases were carried out by DIAMOND method. A total of 93,877 Unigenes had significantly hit on at least one target database (Table 4). The statistics of E-value, similarity and target species for all Unigenes are shown in Fig. 3. The Unigenes with 0 E-value accounted for 8.01% of the total Unigenes. 47.9% of the Unigenes had similarity with target sequences between 90% and 100%. 27,456 Unigenes were matched to Nr database and most of them (86.48%) aligned to the genome sequence of *S. purpuratus*, which belongs to the same family of Strongylocentrotidae with *S. intermedius*. The next closest matches were found for 1.15% of the sequences from *Saccoglossus kowalevskii*.

In total, 19,905 transcripts were annotated by GO analysis with one or more GO term. All GO terms were divided into three subcategory “biological process”, “cellular component” and “molecular function” (Fig. 4). GO annotation showed that 7080, 1216 and 2999 Unigenes were assigned terms in the biological process, cellular component, and molecular function, respectively. Most of the biological process related genes were involved in biological process, oxidation reduction process and regulation of transcription, DNA-templated. Most of the cellular component related genes were involved in cytoplasm, nucleus, and integral component of membrane. Most of the molecular function related genes were involved in ATP binding, protein binding, metalion binding.

To characterize the functions of transcripts, KEGG categories were also analyzed. In total, 11,558 transcripts were mapped to 312 pathways. Pathway maps showed that six KEGG categories, i.e., organismal systems, metabolism, human diseases, genetic information processing, environmental information processing, cellular processes, were annotated in *S. intermedius* transcriptomes (Fig. 5). The largest number of Unigenes (4344) was associated with metabolic pathways. The next largest category was genetic information processing pathway which contained 3028 Unigenes.

3.3. Analysis of differentially expressed genes

To investigate the transcriptome profile of *S. intermedius* in response

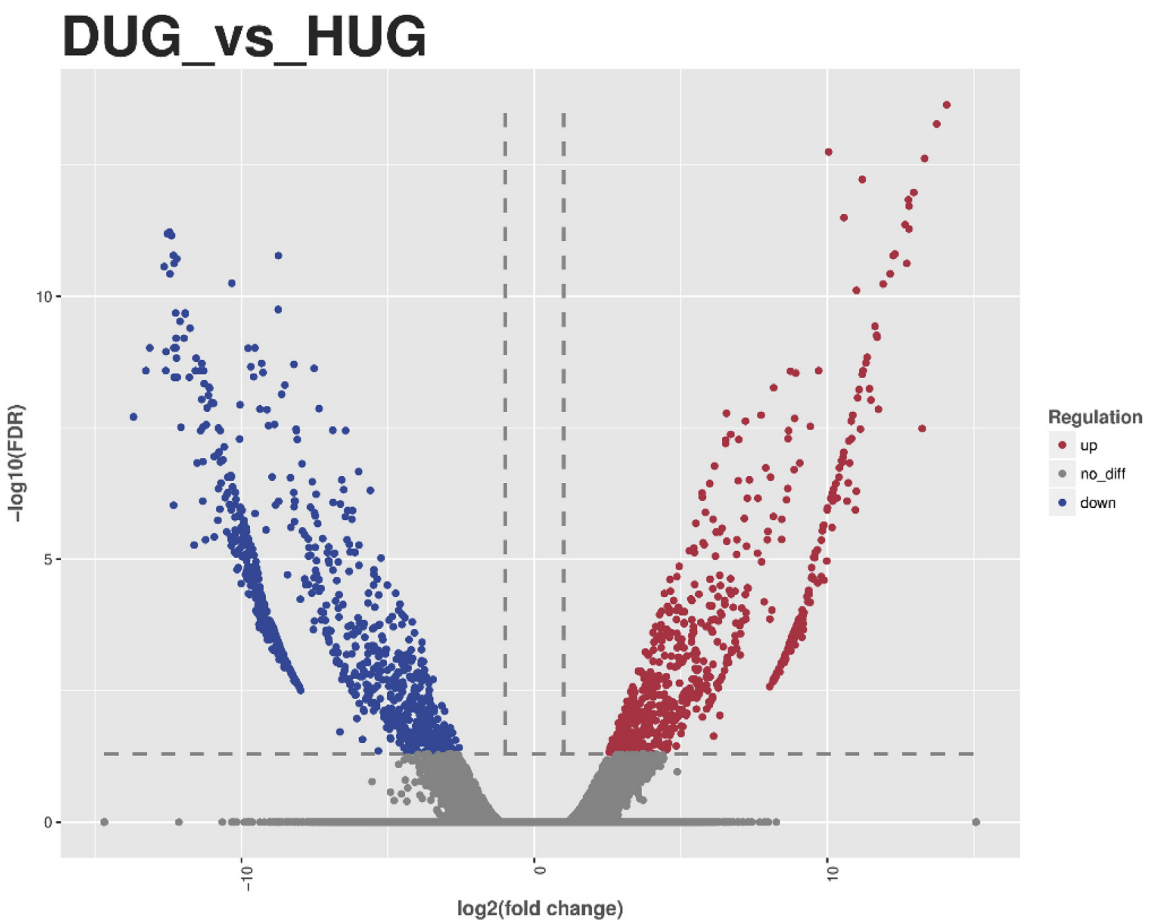

Fig. 6. Differentially expressed genes (DEGs) distribution between spotting diseased sea urchins and healthy ones. The $\log_2$ indicates the mean expression level for each genes. Each dot represents one gene. Red and blue dots represent DEGs. Gray dots represent no differential expressed genes. (For interpretation of the references to color in this figure legend, the reader is referred to the Web version of this article.)

to spotting disease, DEG analysis was performed. Comparisons of gene expression between DUG and HUG identified 1557 DEGs including 689 significantly up-regulated genes and 868 significantly down-regulated genes. The distribution of DEGs and not DEGs are shown in Fig. 6. Heatmap analysis of hierarchical clustering was used to determine the profiles of the DEGs in our research (Fig. 7).

3.4. GO and KEGG enrichment analysis of DEGs

To obtain an overview of the functions of the DEGs in spotting disease, GO and KEGG functional enrichment analysis were performed to identify the main molecular functions of the DEGs involved. The GO pathways that changed significantly between DUG and HUG are list in Supplementary Table 1. The GO functional enrichment analysis of DEGs was classified into three categories, biological process, cellular component and molecular function. The level-3 GO terms in these three categories are showed in Fig. 8a. Lots of immune-related GO terms, such as positive regulation of B cell activity, phagocytosis and recognition, immunoglobulin receptor binding, complement activation, antigen binding, were differently expressed between DUG and HUG. Analysis of KEGG pathway revealed 151 pathways were affected in *S. intermedius* in response to spotting disease. Among them, phagosome and neuroactive ligand-receptor pathways were mostly enriched (Fig. 8b; Supplementary Table 2).

3.5. RT-qPCR validation

To validate the differentially expressed genes identified by RNA-Seq, we analyzed the expression of six genes from the transcriptome data by using RT-qPCR, including CASP8, NCAN, STY46, TIGAR, TRAF3 and TRIM30A. Only one single product was detected for each primer set by dissolve curve analysis. Fold change in HUG and DUG of RT-qPCR were compared with the RNA-Seq expression profiles. All trends of RT-qPCR were correlated with RNA-Seq results, indicating the reliability and accuracy of the assembly and RNA-Seq expression analysis (Fig. 9).

3.6. Discovery of molecular markers

A total of 15,990 SSRs were identified from the assemble sequences. The most abundant type of repeat motifs were dinucleotide repeats (6386), followed by tri- (4724), penta- (362), quad- (329) and hexanucleotide repeats (135) (Fig. 10). A total of 235,249 and 295,567 candidate SNPs were identified from DUG and HUG, respectively (Fig. 11). For DUG, 68,767 were transitions and 97,256 were transversions. For HUG, 173,942 were transitions and 121,625 were transversions. Within transition types, the number of A-G and C-T was similar in both DUG and HUG. The similar results were also observed for the transversion types.

4. Discussion

In this study, 93,877 Unigenes were assembled with an average length of 201 bp, a max length of 16712 bp and a N50 of 1185 bp (Table 2). This N50 is moderate in length among those results from other studies in *S. intermedius* [32–34]. 87,053 Unigenes (92.74%)

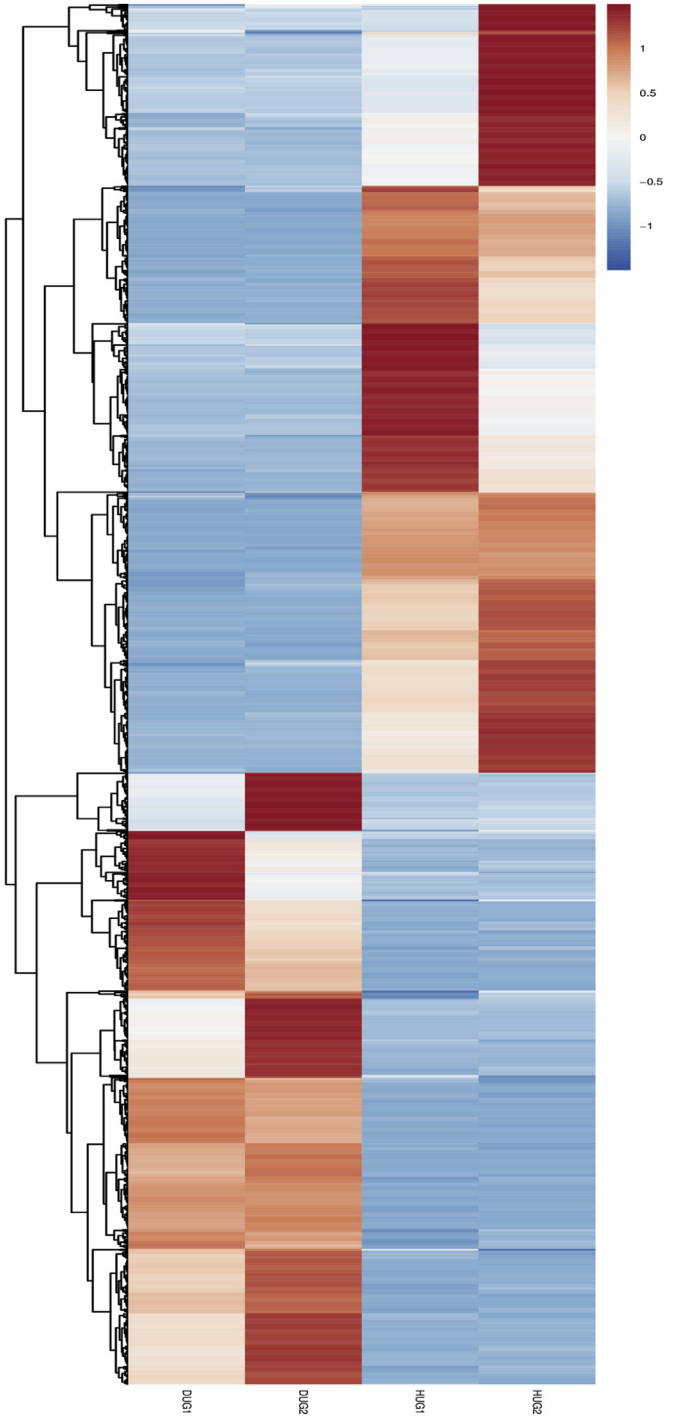

Fig. 7. Heatmap analysis of hierarchical clustering of DEGs in DUG and HUG. Clusters were obtained using the hierarchical-means method based on 1557 DEGs. Each column represents a DUG or HUG sample, and each row represents a gene. Different colors indicate differences in expression. Negative numbers mean down-regulation and positive numbers indicate up-regulation. (For interpretation of the references to color in this figure legend, the reader is referred to the Web version of this article.)

distributed in 200–2000 bp region, while 6824 (7.27%) Unigenes were over 2000 bp in length (Fig. 2). These Unigenes will be very helpful to obtain full-length cDNA. We found that 86.48% of the total 27, 456 Unigenes in *S. intermedius* aligned to the genome sequences of the sea urchin *S. purpuratus* and 1.15% of these Unigenes aligned to the acorn worm *Saccoglossus kowalevskii*. These proportions are comparable with those results by previous studies in *S. intermedius* [33,35] and in another sea urchin species [34]. All these above results suggest the quality of our assembled transcriptome is high.

Two potential causative bacteria had been isolated from spotting diseased sea urchin and were demonstrated to cause spotting disease in some instance (unpublished data). In this study, we collected natural diseased sea urchin with typical syndrome of spotting disease and healthy one (Fig. 1) for transcriptome analysis. We did not perform the bacterial infection experiment to mock the disease outbreak. The main purpose of the present study is to reveal the genes or pathways closely correlated with the spotting disease resistance at transcriptional level. There were 1557 DEGs between HUG and DUG (Figs. 6 and 7) and 151 KEGG pathways were significantly enriched in DEGs. In the same sea urchin *S. intermedius*, Chen et al. [32] performed transcriptome sequencing of different tissues, 54–75 KEGG pathways were significantly enriched in 1247–1784 DEGs. Ding et al. [33] performed transcriptome sequencing of two color tube feet *S. intermedius*, 30–33 pathways were significantly enriched in 881–935 DEGs. Our result discovered more DEGs than the two studies, and more KEGG pathways were enriched in these DEGs. These results suggested a more complex response mechanism in *S. intermedius* to spotting disease than that to different tissue and different tube feet color. It is commonly seen that large number of pathways enriched in DEGs from infected individuals and control ones in aquatic animals. For instance, 92–142 pathways were enriched in DEGs from Chinese white shrimp *Fenneropenaeus chinensis* that infected with WSSV [36] and 266–274 pathways were enriched in DEGs from Japanese flounder *Paralichthys olivaceus* challenged with *Edwardsiella tarda* [37,38]. 4858 DEGs were identified from naturally diseased (skin ulceration syndrome) sea cucumber *Apostichopus japonicus* [39], while only 385–548 DEGs were found from individuals with different growth rate [40]. Abundant immune-related genes such as CASP8,NLRC3,NLRP12, HSP90, macrophage mannose receptor, were annotated. The predominantly enriched GO terms, such as positive regulation of B cell activity, phagocytosis and recognition, immunoglobulin receptor binding, complement activation, antigen binding, were immunologically relevant (Fig. 8a). Similarly, abundant immune-related KEGG signal pathways such as phagosome, NOD-like receptor signaling pathway, intestinal immune network for IgA production, were significantly enriched (Fig. 8b). These results in immune-related genes and pathways indicated a complicated immune defending reaction in *S. intermedius* when facing spotting disease.

In this study, phagosome pathway was significantly changed between HUG and DUG. The coelomic fluid of sea urchins contains four types of coelomocytes, including phagocytic amoebocytes, vibratile cells, red spherule cells and colorless spherule cells. Among the four coelomocytes, phagocytic amoebocytes accounted for more than 60% of the total cells [41]. As a result, phagocytosis is the major form of the innate immunity in sea urchins. The process that phagocytic amoebocytes phagocytose the invasive pathogens in *S. intermedius* has been well demonstrated [42,43]. It is consisted of four steps including chemotaxis, contact, internalization and digestion. Phagocytic amoebocytes produce bactericides such as lipase, peroxidase, serine protease and hydrogen peroxide (H_2O_2) to decompose the invasive pathogens. V-type proton ATPase is a key gene in phagosome pathway [44,45]. It can hydrolyze ATP and establish a transmembrane proton electrochemical gradient to acidify intracellular and extracellular environment [46]. In phagosome, V-type proton ATPase can increase hydrogen ion (H^+) concentration. H^+ will bind with peroxy radical (O_2^{2-}) to form H_2O_2, which could eliminate the invasive pathogens phagocytosed by phagosome [47]. We detected a significant down regulation in gene expression of V-ATPase in spotting diseased sea urchins (DUG). Theoretically, this down regulation might be caused by difference in phagocytic amoebocyte amounts sampled between HUG and DUG. However, actually, we recently found that DUG urchins will increased their phagocytic amoebocyte numbers slightly compared to the HUG ones ($P < 0.05$, data not published). Consequently, the down regulation in gene expression of V-ATPase suggested that the digestion

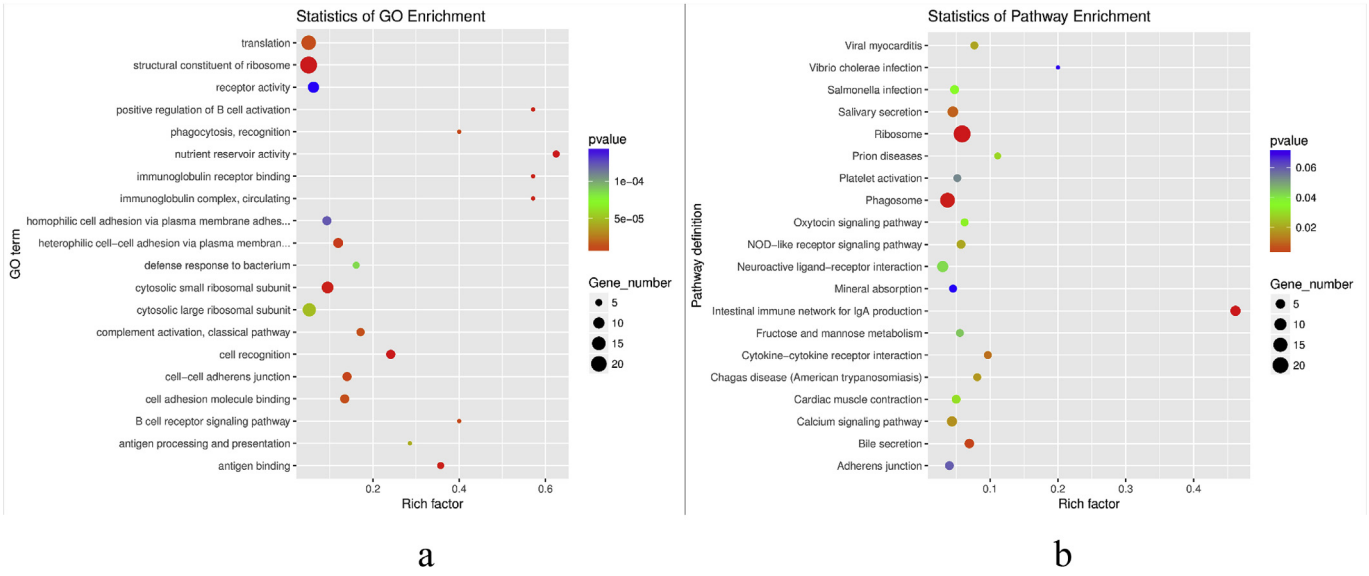

Fig. 8. GO and KEGG enrichment of DGEs. a: GO analysis of DEGs. The x-axis is the rich factor which means the proportion of DEGs in total genes in a GO term. The y-axis is the gene functional classification of GO. Different colors of plots indicate different p values. Plot diameter represents DEG numbers in a GO term; b: KEGG analysis of DEGs. The x-axis is the rich factor which means the proportion of DEGs in total genes in a KEGG term. The y-axis is the gene functional classification of KEGG. Different colors of plots indicate different p values. Plot diameter represents DEG numbers in a KEGG term. (For interpretation of the references to color in this figure legend, the reader is referred to the Web version of this article.)

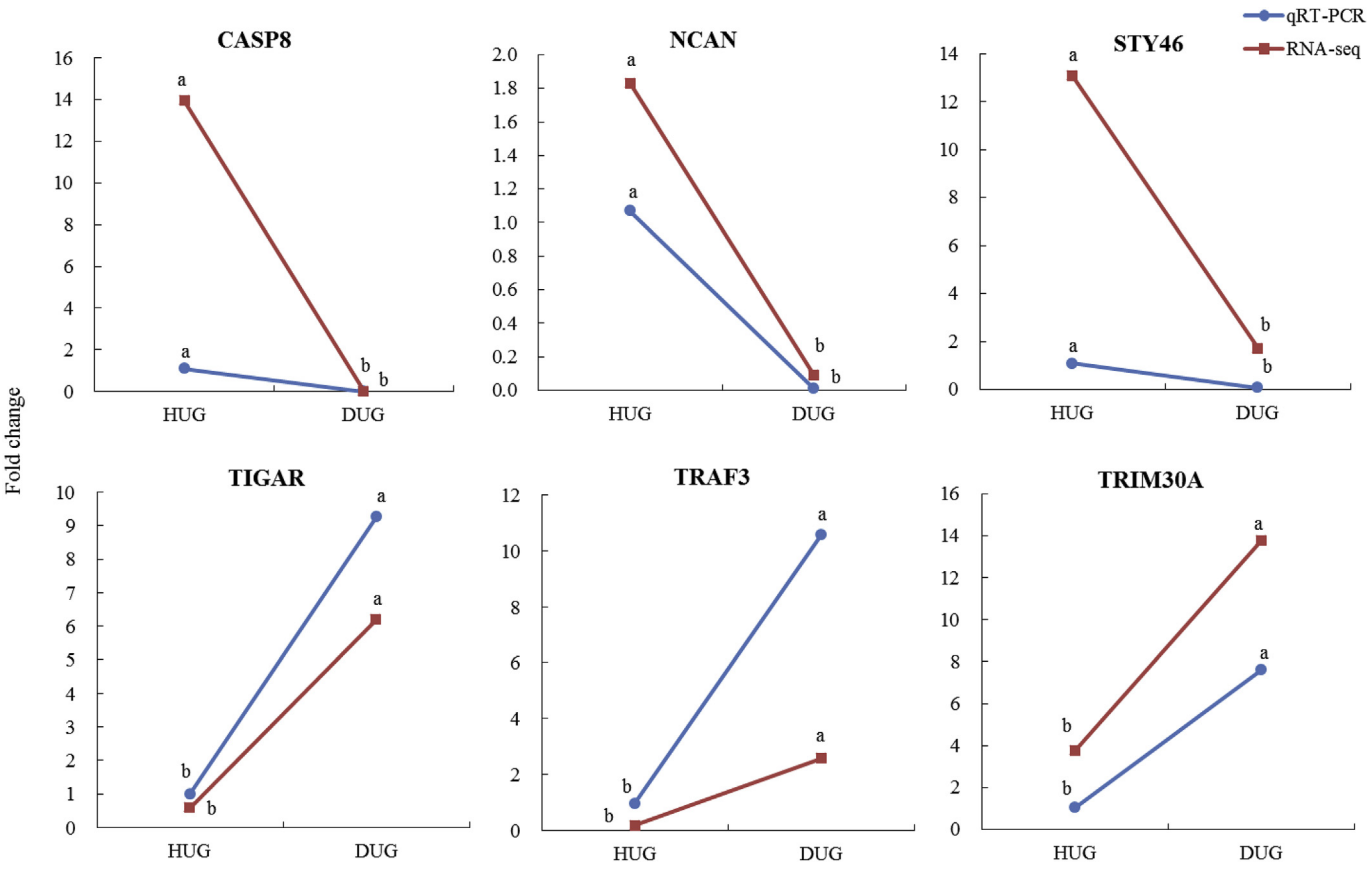

Fig. 9. Confirmation of DGEs expression by RT-qPCR. Expression of the selected DEGs is normalized to that of the *β*-actin gene. The letters a and b indicate significantly expression levels between HUG and DUG.

function of phagosomes in diseased individuals should be inhibited, while the phagosomes in healthy urchins should have more ability to digest the invasive pathogens.

NOD-like receptor signaling pathway is involved in foreign pathogens recognition and downstream pathway activation to simulate immune response. The nucleotide-binding domain and leucine-rich repeat containing gene family (NLR) is an important member of the pattern recognition receptor that exists in cytoplasm and can recognize

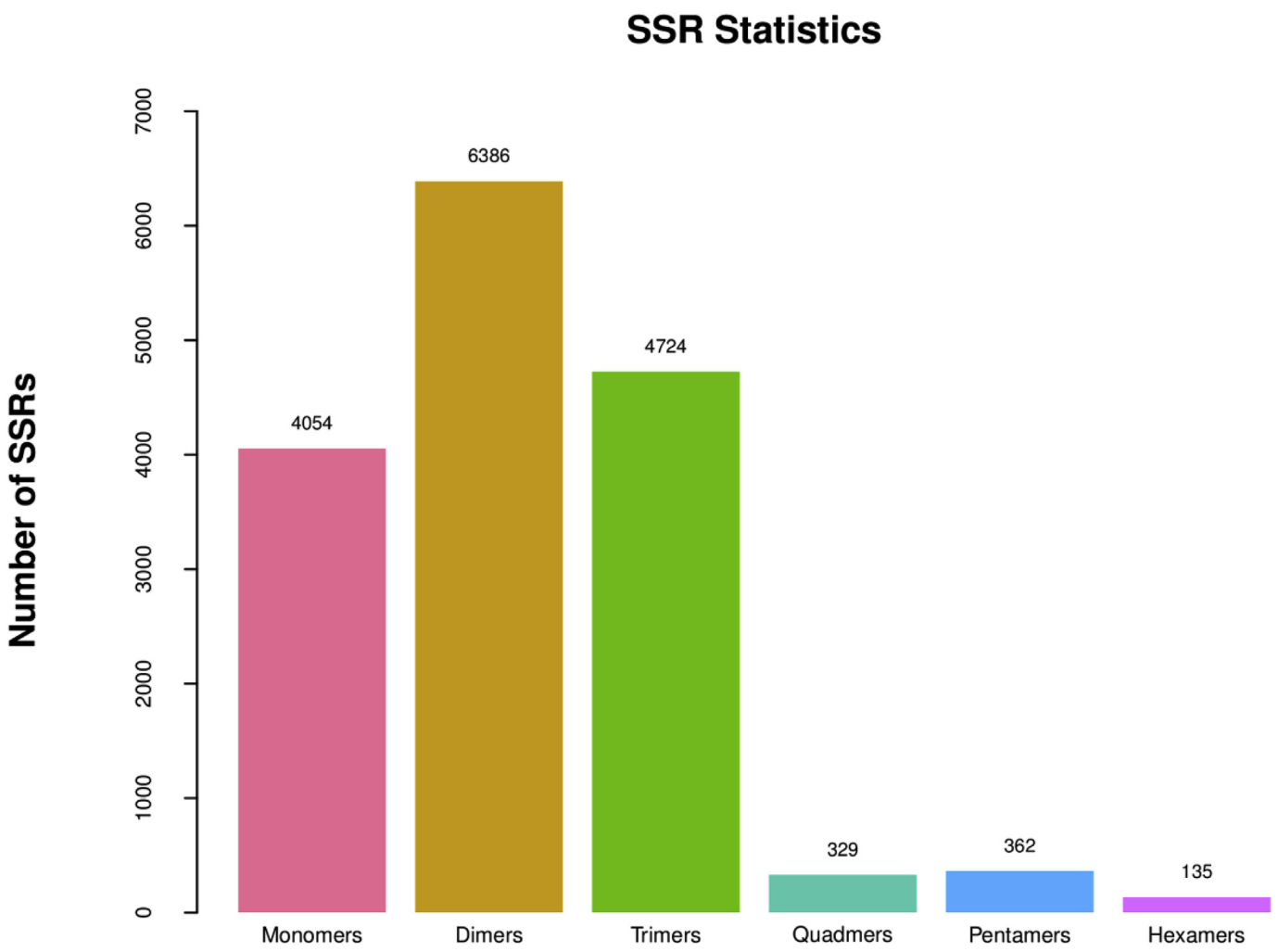

Fig. 10. Length distribution of SSRs based on the number of repeat units of *S. intermedius*. The x-axis is the SSR types.

the foreign antigens including bacterial components, peptidoglycan and nucleic acids. A large number (208) of NLR genes had been found in the genome sequence of *S. purpuratus* [19]. In *S. intermedius*, 9 fragment groups of NLR genes containing more than 80 sequences had been cloned [35], indicating that NLR gene family played an important role in the innate immune system of the sea urchin. In this study, gene expressions of two NLRs, i.e., NLRC3 and NLRP12, were significantly down regulated in diseased sea urchins. NLRP12 is an inhibitory NLR protein can promote the degradation of NIK possibly through interactions with TRAF3 [48,49]. Also, NLRC3 has been reported to negatively affect the activation of NF-κB by negatively affected endotoxin signaling by associating with TRAF6 [50] hence inhibit the inflammatory responses. In HUG, significant higher expression of these two inhibitory NLR proteins than in DUG indicated that the inflammatory responses in healthy urchins had been inhibited. The inhibition might play an important role in maintaining the homeostasis of the body.

Except for the above genes, Toll-like receptor genes, 185/333 gene families and complement C3 genes are also recognized as key genes in sea urchins immunity [19,51,52]. However, these genes had not been well enriched in KEGG pathways. We suppose these genes might play a role in the early phase of the spotting disease infection or might not be essential for resisting the spotting disease. As such, further studies should be conducted.

We identified a large number of SSRs and SNPs which can be used in marker-assisted selection for spotting disease resistance traits in *S. intermeidus*. These results are a database that can supplement our recent study in QTL mapping for growth traits and gonad color [4]. The next important step is to identify candidate genes responsible for spotting disease resistance though locating significant markers along the chromosomes.

In conclusion, we sequenced four transcriptomes of *S. intermedius* and identified 1557 DEGs between naturally spotting diseased sea urchins and healthy individuals. The reliability and accuracy of the assembly and RNA-seq expression analysis were confirmed by RT-qPCR results. Important immune pathways such as phagosome pathway and NOD-like receptor signaling pathway were downregulated, indicating that spotting disease decreased immunity functions of *S. intermedius*, and these pathways might play key roles in spotting disease resistance. Moreover, we identified a large number of SSRs and SNPs which may provide a basis for genetic map construction and QTL mapping for disease resistance trait.

Conflicts of interest

The authors declare no competing financial interest.

Acknowledgments

This work was supported by a Grant for Chinese Outstanding Talents in Agricultural Scientific Research, Agricultural Research and Industrialization Project of Liaoning Province (2015203003), and the K. C. Wong Magna Fund in Ningbo University.

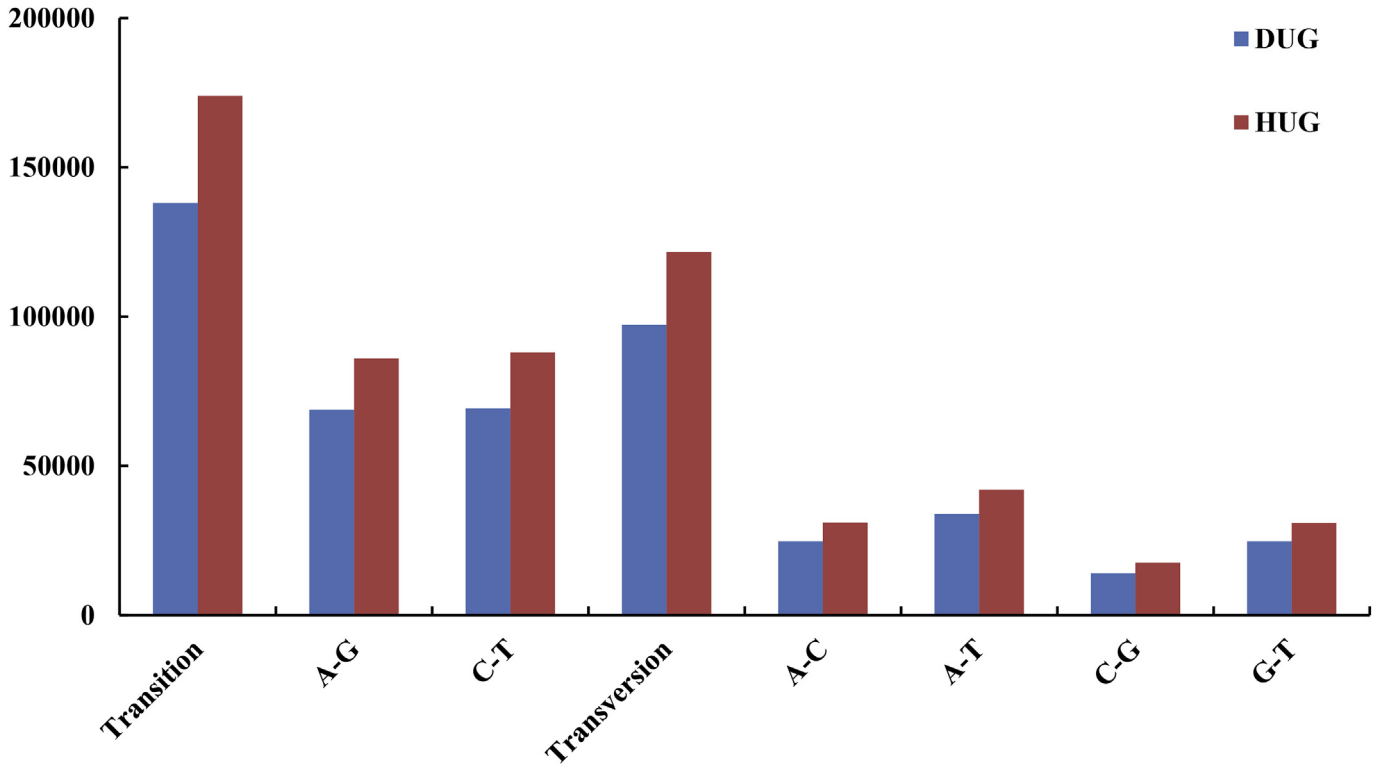

Fig. 11. Distribution of SNPs identified based on diseased sea urchin group (DUG) and healthy sea urchin group (HUG) in *S. intermedius.* The x-axis is the SNP types.

Appendix A. Supplementary data

Supplementary data to this article can be found online at https://doi.org/10.1016/j.fsi.2018.10.042.

References

[1] Y. Chang, J. Ding, J. Song, et al., Biology and Aquaculture of Sea Cucumbers and Sea Urchins, Ocean press, Beijing, China, 2004, p. 217 (In Chinese).
[2] H. Liu, Y. Chang, Sea urchin aquaculture in China, in: N.P. Brown, S.D. Eddy (Eds.), Echinoderm Aquaculture, C.O.S. Printers Pte Ltd, Singapore, 2015, pp. 127–146.
[3] T. Unuma, Y. Sakai, Y. Agatsuma, T. Kayaba, Sea urchin aquaculture in Japan, in: N.P. Brown, S.D. Eddy (Eds.), Echinoderm Aquaculture, C.O.S. Printers Pte Ltd, Singapore, 2015, pp. 77–126.
[4] Y. Chang, J. Ding, Y. Xu, et al., SLAF-based high-density genetic map construction and QTL mapping for major economic traits in sea urchin *Strongylocentrotus intermedius*, Sci. Rep. UK 8 (2018) 820.
[5] Z. Wang, Y. Chang, Studies on hatching of Japanese sea urchin *Strongylocentrotus intermedius*, J. Fish. Sci. China 4 (1997) 60–67 (In Chinese).
[6] W. Zhang, C. Zhao, M. Chen, et al., Family growth response to different laboratory culture environments shows genotype–environment interaction in the sea urchin *Strongylocentrotus intermedius*, Aquacult. Res. 44 (2013) 1706–1714.
[7] W. Zhang, Z. Chong, P. Liu, et al., First report on tube feet differential pigmentation in the cultivated sea urchin *Strongylocentrotus intermedius* (Agassiz, 1863) and its relationship with growth performance: tube feet differential pigmentation in sea urchins, Aquacult. Res. 41 (2010) e706–e708.
[8] Y. Chang, W. Zhang, C. Zhao, et al., Estimates of heritabilities and genetic correlations for growth and gonad traits in the sea urchin *Strongylocentrotus intermedius*, Aquacult. Res. 43 (2012) 271–280.
[9] Y. Chang, Z. Wang, The raft culture of the sea urchin *Strongylocentrotus intermedius*, J. Dalian Fish. Univ. 12 (1997) 7–14 (In Chinese).
[10] Z. Zhou, Z. Bao, Y. Dong, et al., AFLP analysis in populations of *Strongylocentrotus intermedius, S. nudus* and hybrids (*S. intermedius x S. nudus*), Hereditas 29 (2007) 443–448 (In Chinese).
[11] Y. Zhan, W. Hu, W. Zhang, et al., The impact of CO2-driven ocean acidification on early development and calcification in the sea urchin *Strongylocentrotus intermedius*, Mar. Pollut. Bull. 112 (2016) 291–302.
[12] K. Tajima, T. Hirano, K. Nakano, et al., Taxonomical study on the causative bacterium of spotting disease of sea urchin *Strongylocentrotus intermedius*, Fish. Sci. 63 (1997) 897–900.
[13] K. Tajima, T. Hirano, M. Shimizu, et al., Isolation and pathogenicity of the causative bacterium of spotting disease of sea urchin *Strongylocentrotus intermedius*, Fish. Sci. 63 (1997) 249–252.
[14] K. Tajima, K. Takeuchi, I.M. Mahbub, et al., Studies on a bacterial disease of sea urchin *Strongylocentrotus intermedius* occurring at low water temperatures, Fish. Sci. 64 (1998) 918–920.
[15] K. Takeuchi, K. Tajima, I.M. Mahbub, et al., Taxonomical and serological studies on the causative bacteria of the disease of sea urchin *Strongylocentrotus intermedius* occurring at low water temperatures, Fish. Sci. 65 (1999) 264–268.
[16] Y. Wang, Y. Chang, J.M. Lawrence, Disease in sea urchin, in: J.M. lawrence (Ed.), Sea Urchins: Biology and Ecology, 3 ed., Elsevier, United Kingdom, 2013, pp. 179–186.
[17] B. Wang, Y. Li, X. Li, et al., Pathogenic mechanism of the causative vibrio found in "red spotting" diseased sea urchin *Strongylocentrotus intermedius*, J. Dalian Fish. Univ. 20 (2005) 11–15 (In Chinese).
[18] B. Wang, Y. Li, X. Li, et al., Biological characteristic and pathogenicity of the pathogenic vibrio on the "red spot disease" of *Strongylocentrotus intermedius*, J. Fish. China 30 (2006) 371–376 (In Chinese).
[19] E. Sodergren, G.M. Weinstock, E.H. Davidson, et al., The genome of the sea urchin *Strongylocentrotus purpuratus*, Science 314 (2006) 941–952.
[20] S.V. Nair, V.H. Del, P.S. Gross, et al., Macroarray analysis of coelomocyte gene expression in response to LPS in the sea urchin. Identification of unexpected immune diversity in an invertebrate, Physiol. Genom. 22 (2005) 33–47.
[21] M. Shah, K.M. Brown, L.C. Smith, The gene encoding the sea urchin complement protein, SpC3, is expressed in embryos and can be upregulated by bacteria, Dev. Comp. Immunol. 27 (2003) 529–538.
[22] Y. Wang, J. Ding, Y. Liu, et al., Isolation of immune-relating 185/333-1 gene from sea urchin (*Strongylocentrotus intermedius*) and its expression analysis, J. Ocean Univ. China 15 (2016) 163–170.
[23] Y. Wang, N. Feng, Q. Li, et al., Isolation and characterization of bacteria associated with a syndrome disease of sea urchin *Strongylocentrotus intermedius* in North China, Aquacult. Res. 44 (2013) 691–700.
[24] Y. Wang, S. Cheng, Y. Chang, et al., Identification and expression analysis of a TLR11 family gene in the sea urchin *Strongylocentrotus intermedius*, Immunogenetics 70 (2018) 337–346.
[25] M. Martin, Cutadapt removes adapter sequences from high-throughput sequencing reads, EMBnet J. 17 (2011) 10–12.
[26] M.G. Grabherr, B.J. Haas, M. Yassour, et al., Full-length transcriptome assembly from RNA-Seq data without a reference genome, Nat. Biotechnol. 29 (2011) 644–652.
[27] B. Buchfink, C. Xie, D.H. Huson, Fast and sensitive protein alignment using DIAMOND, Nat. Methods 12 (2015) 59.
[28] R. Patro, G. Duggal, M.I. Love, et al., Salmon provides fast and bias-aware quantification of transcript expression, Nat. Methods 14 (2017) 417–419.
[29] A. Mortazavi, B. Williams, K. McCue, et al., Mapping and quantifying mammalian transcriptomes by RNA-seq, Nat. Methods 5 (2008) 621.
[30] M.D. Robinson, D.J. Mccarthy, G.K. Smyth, edgeR: a Bioconductor package for differential expression analysis of digital gene expression data, Bioinformatics 26 (2010) 139.
[31] K. Livak, T. Schmittgen, Analysis of relative gene expression data using real-time

quantitative PCR and the $2^{-\Delta\Delta CT}$ method, Methods 25 (2001) 402–408.
[32] Y. Chen, Y. Chang, X. Wang, et al., De novo assembly and analysis of tissue-specific transcriptomes revealed the tissue-specific genes and profile of immunity from *Strongylocentrotus intermedius*, Fish Shellfish Immunol. 46 (2015) 723–736.
[33] J. Ding, D. Yang, Y. Chang, et al., Comparative transcriptome analysis of tube feet of different colors in the sea urchin *Strongylocentrotus intermedius*, Gene Genom. 39 (2017) 1215–1225.
[34] G.B. Gillard, D.J. Garama, C.M. Brown, The transcriptome of the NZ endemic sea urchin Kina (*Evechinus chloroticus*), BMC Genomics 15 (2014) 45.
[35] Y. Chen, X. Liu, Y. Chang, et al., Cloning of partial sequence and expression of NLR family in sea urchin *Strongylocentrotus intermedius*, J. Dalian Ocean Univ. 29 (2014) 336–341 (In Chinese).
[36] X. Shi, X. Meng, J. Kong, et al., Transcriptome analysis of 'Huanghai No. 2' *Fenneropenaeus chinensis* response to WSSV using RNA-seq, Fish Shellfish Immunol. 75 (2018) 132–138.
[37] Z. Li, X. Liu, J. Liu, et al., Transcriptome profiling based on protein-protein interaction networks provides a core set of genes for understanding blood immune response mechanisms against Edwardsiella tarda infection in Japanese flounder (*Paralichthys olivaceus*), Dev. Comp. Immunol. 78 (2017) 100–113.
[38] Z. Li, X. Liu, J. Cheng, et al., Transcriptome profiling provides gene resources for understanding gill immune responses in Japanese flounder (*Paralichthys olivaceus*) challenged with *Edwardsiella tarda*, Fish Shellfish Immunol. 72 (2017) 593–603.
[39] P. Zhang, C. Li, L. Zhu, et al., De novo assembly of the sea cucumber *Apostichopus japonicus* hemocytes transcriptome to identify miRNA targets associated with skin ulceration syndrome, PLoS One 8 (2013) e73506.
[40] L. Gao, C. He, X. Bao, et al., Transcriptome analysis of the sea cucumber (*Apostichopus japonicus*) with variation in individual growth, PloS One 12 (2017) e0181471.
[41] K. Bertheussen, R. Seljelid, Echinoid phagocytes in vitro, Exp. Cell Res. 111 (1978) 401–412.
[42] X. Li, B. Wang, J. Liu, et al., Type and function of coelomocyte in sea urchin *Strongylocentrotus intermedius*, J. Fish. Sci. China 10 (2003) 381–385 (In Chinese).
[43] Y. Zhang, D. Li, Y. Chang, et al., Study of opsonin-like molecule from coelomic fluid of *Strongylocentrotus intermedius*, J. Fish. China 38 (2014) 690–696 (In Chinese).
[44] G.H. Sunwada, Y. Wada, M. Futai, Lysosome and lysosome-related organelles responsible for specialized functions in higher organisms, with special emphasis on vacuolar-type proton ATPase, Cell Struct. Funct. 28 (2003) 455–463.
[45] T. Wassmer, M. Froissard, H. Plattner, et al., The vacuolar proton-ATPase plays a major role in several membrane-bounded organelles in *Paramecium*, J. Cell Sci. 118 (2005) 2813–2825.
[46] S. Wilkens, Z. Zhang, Y. Zheng, A structural model of the vacuolar ATPase from transmission electron microscopy, Micron 36 (2005) 109–126.
[47] T. Nishi, M. Forgac, The vacuolar (H+)-ATPases–nature's most versatile proton pumps, Nat. Rev. Mol. Cell Biol. 3 (2002) 94–103.
[48] I.C. Allen, J.E. Wilson, M. Schneider, et al., NLRP12 suppresses colon inflammation and tumorigenesis through the negative regulation of non-canonical NF-κB signaling and MAP kinase activation, Immunity 36 (2012) 742–754.
[49] X. Xia, J. Cui, H.Y. Wang, et al., NLRX1 negatively regulates TLR-induced NF-κB signaling by targeting TRAF6 and IKK, Immunity 34 (2011) 843–853.
[50] M. Schneider, A.G. Zimmermann, R.A. Roberts, et al., The innate immune sensor NLRC3 attenuates Toll-like receptor signaling via modification of the signaling adaptor TRAF6 and transcription factor NF-κB, Nat. Immunol. 13 (2012) 823–831.
[51] L.C. Smith, Diversification of innate immune genes: lessons from the purple sea urchin, Dis. Mod. Mec. 3 (2010) 274.
[52] L.C. Smith, J.P. Rast, V. Brockton, et al., The sea urchin immune system, ISJ-Invert Surviv J. 3 (2006) 217–224.